

DETECTION OF FOULING IN A CROSS-FLOW HEAT EXCHANGER USING WAVELETS

H. Ingimundardóttir¹ and S. Lalot^{2,3}

¹ University of Iceland, Hjarðarhaga 2-6, 107 Reykjavik, Iceland

² Univ Lille Nord de France, F-59000 Lille, France

³ UVHC, LME, F-59313 Valenciennes, France

sylvain.lalot@univ-valenciennes.fr (corresponding author)

ABSTRACT

Detection of fouling in a heat exchanger experiencing perfect steady state conditions is not very difficult. But the challenge is to detect fouling when all inputs (inlet temperature of the fluids as well as the mass flow rates) are simultaneously varying. In this paper it has been considered that the mass flow rates can vary in a ratio of 2, and that the inlet temperatures can vary by about +/- 20%. This first approach is dedicated to show the feasibility of using the wavelet transform. So, it has been considered that getting simulated data is the best way. In fact, it is then possible to introduce an arbitrary fouling factor. Thus, in the first part of the paper the model of the heat exchanger is presented. It is developed using Simulink. The validation is carried out on an electrical heater, for which it is possible to find an analytical solution for transient states. It is also shown that steady states are accurately computed over a large range of the number of transfer units and heat capacity rate ratios. Then a brief overview of the wavelet transform is given. Then basic examples show that the wavelet transform can help to find the trend of time series. It is then applied to the analysis of the "wavelet transformed" effectiveness of the heat exchanger. This analysis is carried out on a sliding observation window (to be able to detect fouling online). It is shown that fouling is detected at a very early stage.

INTRODUCTION

Studies concerning fouling can be divided in three complementary domains: the principles of fouling (chemistry and flow conditions, e.g. (Rosmaninho et al., 2008) or (Guérin et al., 2007), the mitigation of fouling (design phase, water treatment, surface treatment,..., e.g. (Kukulka and Devgun, 2007) or (Rosmaninho et al., 2007), and fouling monitoring (model based techniques, sensors, ...), e.g. (Prieto et al., 2000) (Riverol and Napolitano, 2002) (Lalot and Lecoeuche, 2003) (Jonsson et al., 2007) (Lalot et al. 2007) (Delmotte et al., 2008) (Mercère et al. 2009). The present study belongs to the last category: online fouling monitoring. It is not a model based technique such as the one presented in (Lalot, 2006, part 1 and 2) or in (Lalot and Mercère, 2008). It is only based on the evolution analysis of the effectiveness of the heat exchanger.

But it is well known that in transient states, the effectiveness of a heat exchanger is not defined. That is why

it has been necessary first to find a tool able to determine a sliding average "steady state" of the heat exchanger. After a first test of the simple "slope method" presented in (Gudmundsson et al., 2008), it has been chosen to try a more complex tool, a wavelet transformation, as it is used in many fields, see e.g. (Prabhakar et al., 2002) (Lou and Loparo, 2004) (Purushothamet al., 2005) (Li, 2009) (Wu et al., 2009) (Wu and Liu, 2009). A wavelet transform is basically a signal processing tool (see e.g. (Heneghan et al., 1994) (Farooq and Datta, 2003)) and will be introduced in this paper after the presentation of the heat exchanger model.

THE HEAT EXCHANGER

To be able to evaluate the efficiency of the method proposed here, it has been chosen to work using simulated data. In this case, it is possible to introduce an arbitrary time variation of the fouling factor; and consequently to know what this factor is when fouling is detected. The next subsection is dedicated to the description of the heat exchanger.

Description of the Heat Exchanger

It has been chosen to model a cross-flow heat exchanger, having both fluids unmixed. The fluids are separated by a plate; the other side of the fluid channels being perfectly insulated. To model the exchanger using Simulink, it is necessary to divide it in "cells" as shown in figure 1.

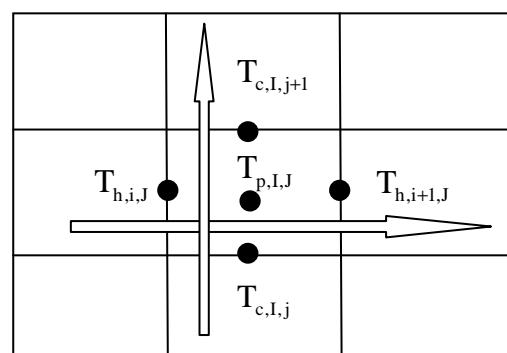


Fig. 1 Discretization of the heat exchanger.

In each cell 3 energy balance equations can be written, one for the hot fluid:

$$M_h c_h \frac{d}{dt} \frac{T_{h,i,J} + T_{h,i+1,J}}{2} = \dot{m}_{h,J} c_h (T_{h,i,J} - T_{h,i+1,J}) + \alpha_{I,J} A_{h,I,J} \left(T_{p,I,J} - \frac{T_{h,i,J} + T_{h,i+1,J}}{2} \right) \quad (1)$$

one for the cold fluid:

$$M_c c_c \frac{d}{dt} \frac{T_{c,I,j} + T_{c,I,j+1}}{2} = \dot{m}_{c,I} c_c (T_{c,I,j} - T_{c,I,j+1}) + \beta_{I,J} A_{c,I,J} \left(T_{p,I,J} - \frac{T_{c,I,j} + T_{c,I,j+1}}{2} \right) \quad (2)$$

and one for the separating plate:

$$M_p c_p \frac{dT_{p,I,J}}{dt} = -\alpha_{I,J} A_{h,I,J} \left(T_{p,I,J} - \frac{T_{h,i,J} + T_{h,i+1,J}}{2} \right) - \beta_{I,J} A_{c,I,J} \left(T_{p,I,J} - \frac{T_{c,I,j} + T_{c,I,j+1}}{2} \right) \quad (3)$$

Introducing, $NUT_{I,J} = \alpha_{I,J} A_{h,I,J} / \dot{m}_{h,J} c_h$ and $nut_{I,J} = \beta_{I,J} A_{c,I,J} / \dot{m}_{c,I} c_c$, that are similar to number of transfer units, $\tau_{h,I,J} = M_h / \dot{m}_{h,J}$ and that are the residence time in one cell, $\gamma_{I,J} = \alpha_{I,J} A_{h,I,J} / M_p c_p$ and $\delta_{I,J} = \beta_{I,J} A_{c,I,J} / M_p c_p$, that are inverses of response times, it is possible to build the respective blocks in Simulink. To do so, it has to be noted that it is better to use integrators than to use derivatives.

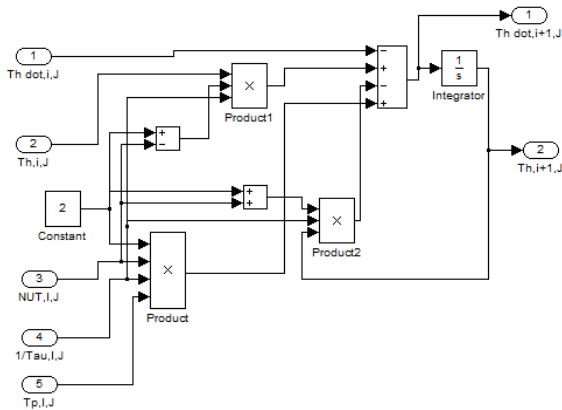


Fig. 2 Simulink block for the hot fluid (one cell)

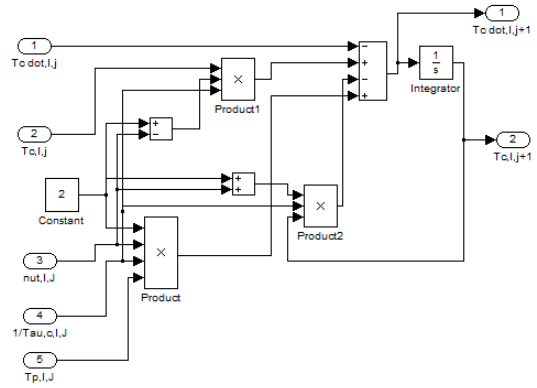


Fig. 3 Simulink block for the cold fluid (one cell)

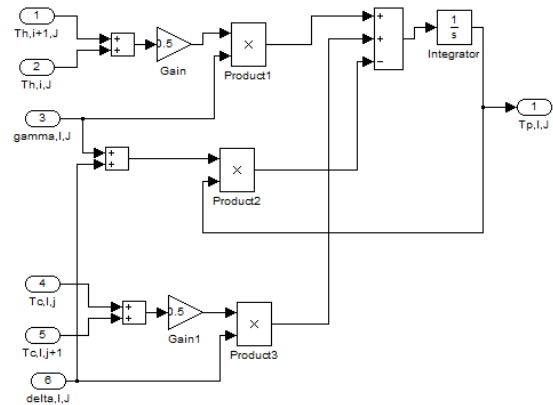


Fig. 4 Simulink block for the separating plate (one cell)

Using these blocks, one cell is defined as described in figure 5.

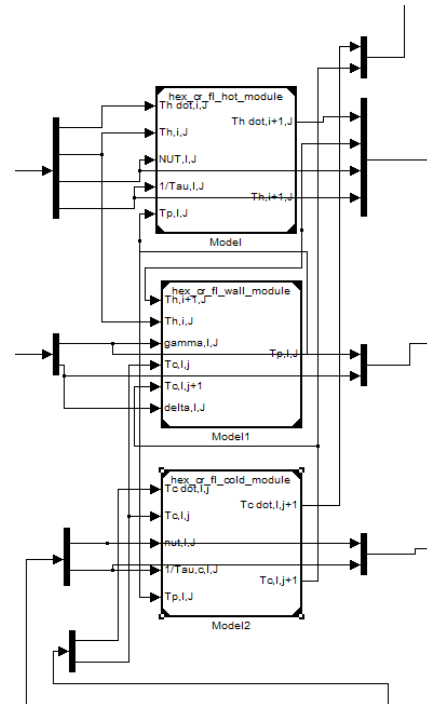


Fig. 5 one cell of the cross-flow heat exchanger

Determination of the cell number

It is then necessary to determine how many cells are to be linked to compute an accurate solution. To do so, it has been decided to model an electrical heater for which an analytical solution can be found. The geometry is quite simple, a thin plate is heated by Joule effect, so that a constant heat flux is generated all along the heater; its length being 1 meter. It is considered that the temperature of the plate is homogeneous in the direction perpendicular to the flow. In this case, the exact solution in the Laplace space is given by eq. 4 for the transfer function.

$$\overline{T}_h = \frac{NTU/\tau}{s(s + NTU/\tau + \gamma)} \times \left\{ 1 - \exp(-\tau s) \exp\left(-NTU \frac{s}{s + \gamma}\right) \right\} \quad (4)$$

where $NTU = hA / \dot{m}_h c_h$, $\tau = M_h / \dot{m}_h$, and $\gamma = hA / M_p c_p$. When applying a step function for the heat flux, the solution is given by eq. 5.

$$T_h = \frac{NTU/\tau}{NTU/\tau + \gamma} \times [1 - \exp(-(NTU/\tau + \gamma)t)] - \frac{NTU}{\tau} \exp(-NTU) \times \left\{ \exp(-(NTU/\tau + \gamma)t) \times \left[\frac{NTU/\tau}{NTU/\tau + \gamma} + \frac{\gamma}{NTU/\tau + \gamma} \right] \right\} * \left(\exp(-\gamma t) \times I_0(2\sqrt{NTU\gamma t}) \right) (t - \tau) \quad (5)$$

It is then possible to compare this analytical solution, to the solution obtained with a Simulink model. Figure 6 shows that choosing 20 cells leads to a very accurate solution. Note that to get this solution, the Simulink block of the plate has been slightly modified to take account of the constant heat flux.

It can be noted that the study of a heat exchanger having a constant plate temperature leads to the same conclusion: 20 cells are sufficient in the flow direction.

It is also important to note that the steady states should be reached whatever the temperature level and the mass flow rates are. This is done comparing the effectiveness computed in a steady state for a large range of Number of Transfer Units values and a large range of heat capacity rate ratios. Figure 7 shows the comparison of analytical results

(see e.g. (Çengel, 1997)) to results obtained using 20 x 20 cell groups (or 1200 blocks) in Simulink.

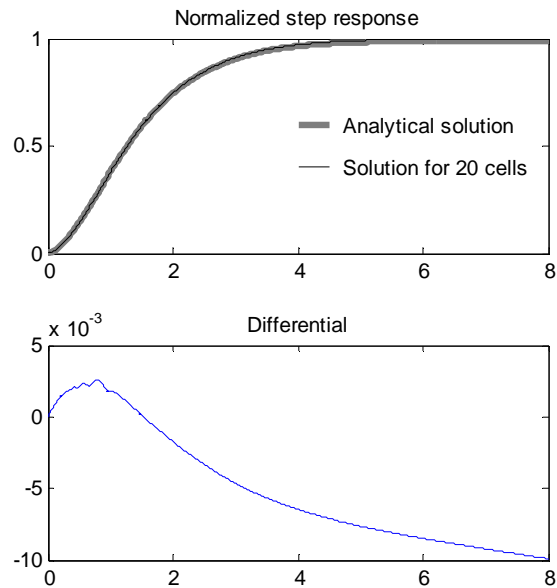


Fig. 6 Comparison of the results obtained using the Simulink model and analytical results (transient state)

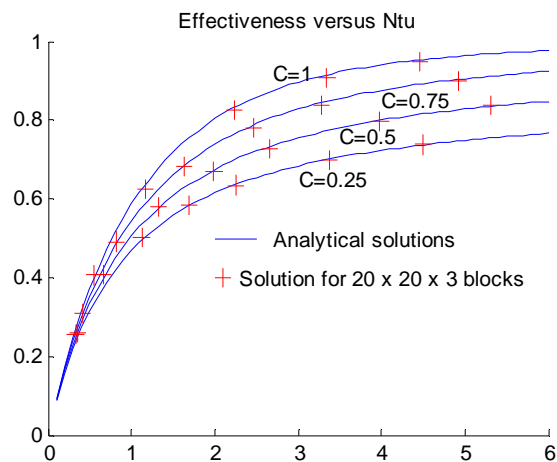


Fig. 7 Comparison of the results obtained using the Simulink model and analytical results (steady states)

THE WAVELET TRANSFORM

A short introduction

When analyzing non-stationary signals it is necessary to take careful consideration to the time and frequency domains and what compromises should be made between the two. Standard Fourier transform is only localized in frequency; the short-time Fourier transform is limited by its fixed window length. On the contrary, wavelets are localized both in time and in frequency; but it is possible to control the localization. Therefore it is foreseen to get a better tool.

In fact, wavelets separate data into frequency components and analyze each component with a resolution matched to its scale. The more the wavelet is similar to the

signal components the larger is the corresponding wavelet coefficient.

Wavelet transform can be beneficial for feature extraction, e.g. fingerprints recognition (Wavelet-based fingerprint image retrieval (Montoya Zegarra et al., 2009), or for diagnosis, e.g. (Sung et al., 2000) (Belotti et al., 2006) (Saravanan and Ramachandran, 2009) (Wu and Chan, 2009).

Wavelets are functions that satisfy certain requirements, e.g. they should integrate to zero, waving above and below the x-axis; be well localized; and other requirements are technical to insure quick and easy calculations to the direct and inverse wavelet transform.

Wavelets are structured basis in discrete or continuous time, and they allow different time versus frequency resolution trade-offs.

Wavelet transforms are built on orthonormal bases of the form $\phi_{jk}(x) = \{2^{j/2} \phi(2^j x - k) : (j, k) \in \mathbb{Z}^2\}$. So, each element of the basis is a translated and dilated version of a single wavelet. Usually, $\phi_{jk}(x)$ are called daughter wavelets of the mother wavelet ϕ . When the mother wavelet is composed of two parts (the lowpass part η and the highpass part μ), any arbitrary signal can be expressed as follows:

$$f(t) = \sum_{k=1}^N \gamma_j(k) \eta(2^j t - k) + \sum_{k=1}^N \lambda_j(k) \mu(2^j t - k)$$

where j fixes the level of approximation available, N fixes the level of approximation used when reconstructing the signal, γ_j are the lowpass coefficients, and λ_j are the highpass coefficients. The latter are computed using the inner product between the original signal and the lowpass part η of the wavelet and the highpass part μ of the wavelet respectively.

For the present study, the Daubechies wavelet basis has been chosen, see e.g. (Daubechies, 1988). It is compactly supported and can be designed with as much smoothness as desired. It relies on the iteration of the discrete filter bank that converges to a continuous time wavelet basis. Daubechies wavelets are designed so that they have the minimum length of support for a given number of vanishing points. Note that when the support is short, the wavelet does not interact very much with a singularity. In this case, two parameters are necessary. The first parameter, *dim*, is the length of the support; the second parameter, *scale*, fixes the approximation level.

Figure 8 shows the lowpass and highpass parts for 16 sample long support.

For a longer introduction to wavelets, see e.g. <http://users.rowan.edu/~polikar/WAVELETS/WTtutorial.html>

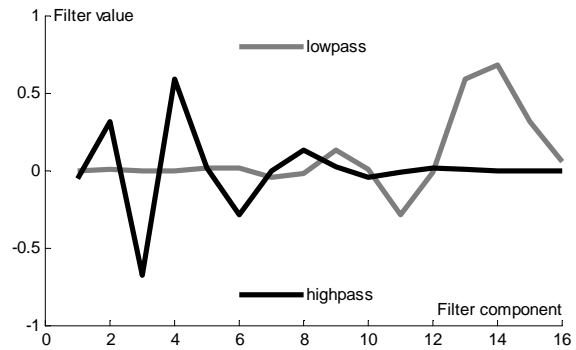


Fig. 8 Filter values (lowpass and highpass filters)

Illustrative example

It is interesting to show the influence of the two main parameters used in the wavelet transform. Figure 9 shows for 2 values of the parameter *dim* and for 4 values of the parameter *scale*, the result of the approximation process on an arbitrary signal.

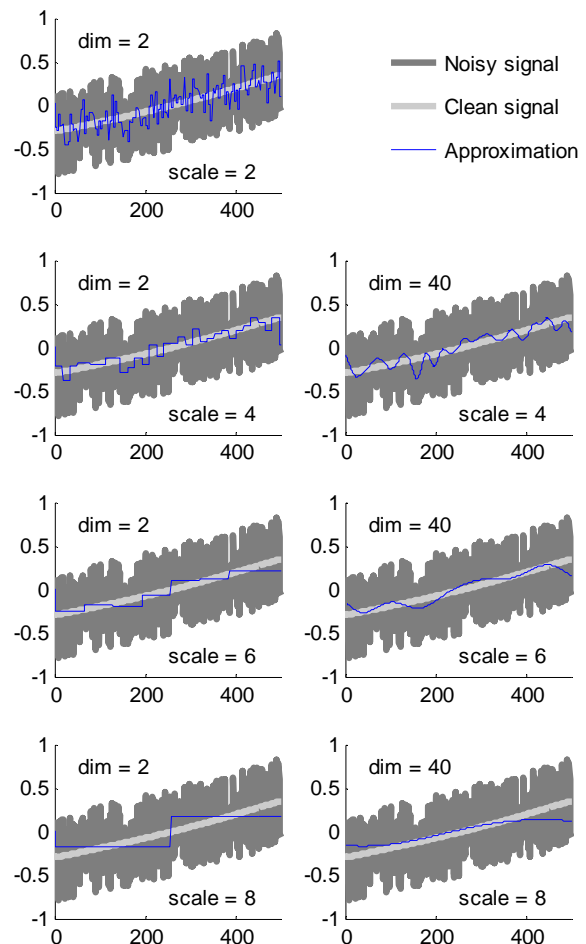


Fig. 9 Illustration of the wavelet transform process

It can be seen that the couple $(dim, scale)=(2,6)$ would lead to an easy detection for this set of data. These values are chosen as starting points for fouling detection.

RESULTS

In a first step, 200 sets of data have been generated. The first half are for a clean exchanger; the second half are for a heat exchanger where fouling occur. In all cases, the following ranges are used:

- 0.6 to 1.2 kg/s for the mass flow rates
- 16 to 24°C for the inlet temperature of the cold fluid
- 56 to 64°C for the inlet temperature of the hot fluid

The values are randomly varying (from time 0 to time 10 000 seconds), as shown in figure 10 (partial view).

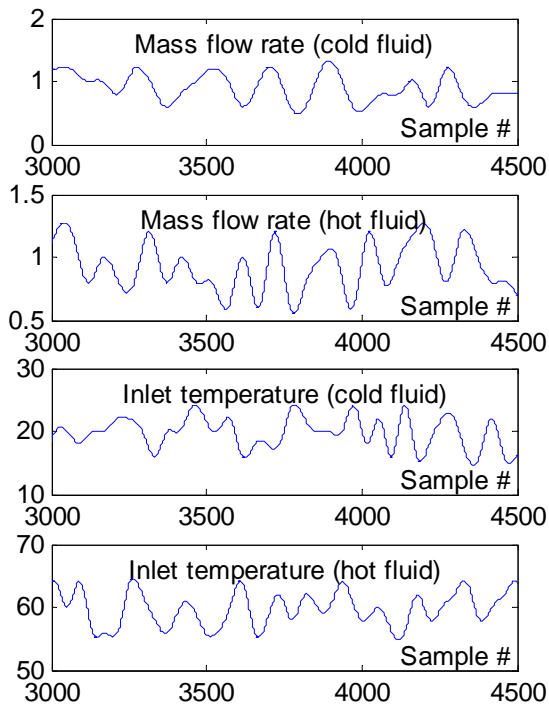


Fig. 10 Partial view of the inputs (set #80)

During this period the fouling factor increases (applied on the hot side). Figure 11 shows this evolution.

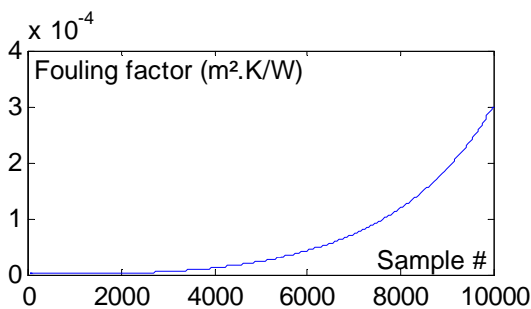


Fig. 11 Evolution of the fouling factor (all sets)

The corresponding outlet temperatures are shown in figure 12. Note that for a given "clean" set, the corresponding "fouling" set takes account of exactly the same inputs.

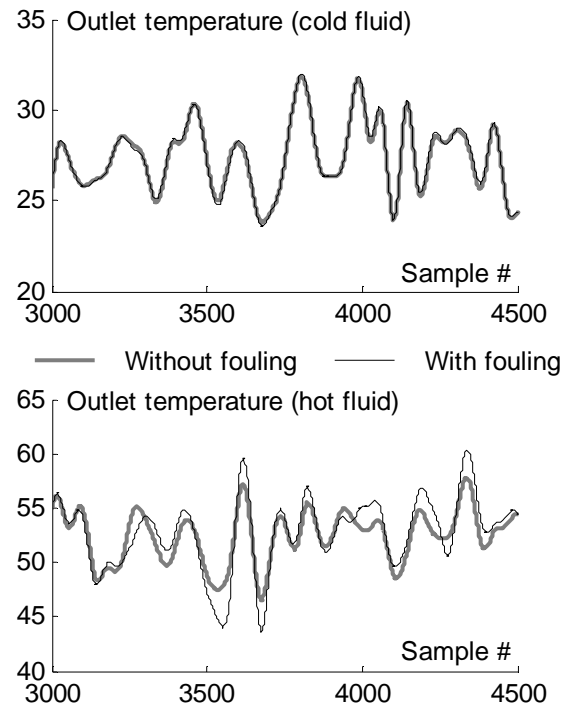


Fig. 12 Partial view of the hot and cold fluids outlet temperature (set #80)

In a second step, an analysis is carried out. Figure 13 shows that it is not possible to try to detect fouling using the raw evolution of an "instantaneous effectiveness". The latter would be defined as the instantaneous value of the classical effectiveness (the ratio of the actual heat transfer rate to the maximum heat transfer rate).

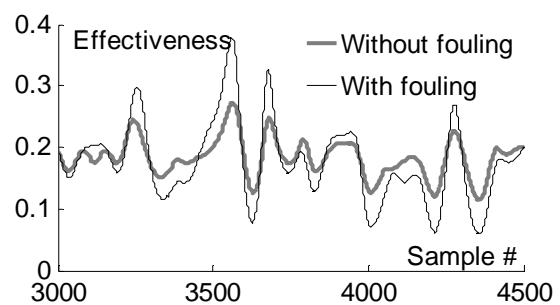


Fig. 13 Partial view of the evolution of an "instantaneous effectiveness" (set #80)

Figures 12 and 13 clearly show the effect of fouling. The heat transfer being reduced, the effect of the thermal inertia of the plate becomes stronger. Hence, the filtering effect (from the hot side to the cold side) is stronger, and the outlet temperature of the cold fluid is nearly not affected by fouling. For the hot fluid, when, without fouling, the outlet temperature begins to decrease, fouling delays this cooling effect. Hence, the outlet temperature is higher with fouling than without fouling, leading to a higher effectiveness. A similar phenomenon occurs when the outlet temperature of the hot fluid would increase (without fouling). Fouling

increases the delay, and the outlet temperature of the hot fluid goes on decreasing, lowering the effectiveness.

Figure 14 shows the procedure used to detect fouling. The first thousand samples are skipped, just to show that the analysis can be applied on an ongoing process. The next samples (in the sliding observation window) are used to compute the approximation of the effectiveness. On these samples, the wavelet transform is applied to the instantaneous effectiveness. To avoid the "side effect" seen on figure 8, it has been chosen to consider only 85% of the computed values. The average value obtained over this interval is considered to be the reference value; then the ratio of the approximated effectiveness to this average value is plotted. The upper bound of the observation window is moved by an offset, and the same procedure is applied (wavelet transform+average value+ratio). In this study, the first computed value is calculated for sample number 6500, to be able to detect fouling when the fouling factor is just higher than $0.55 \times 10^{-4} \text{ m}^2\text{K/W}$. As fouling is quite slow, the offset is set to 200 samples.

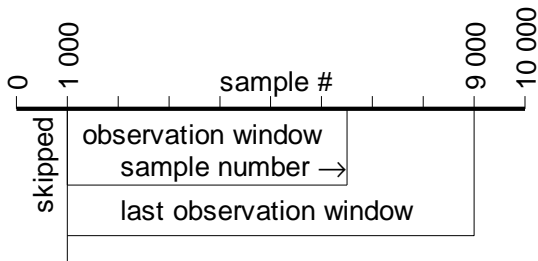


Fig. 14 Effectiveness ratio computation procedure

Figure 15 shows the evolutions of the effectiveness ratio for the 100 "clean" heat exchangers, and for the 100 "fouling" heat exchangers. A very simple test is then carried out. As soon as the effectiveness ratio is lower than a threshold, it is said that fouling occurs. It can be seen on figure 14 that choosing 0.88 as the threshold leads to no false alarm, and that fouling is detected for the 100 "fouling" heat exchangers. In the latter case, fouling is detected at sample 6500 for 93 tests, and at sample 7300 for 7 tests. This corresponds to fouling factors of $0.55 \times 10^{-4} \text{ m}^2\text{K/W}$ and $0.83 \times 10^{-4} \text{ m}^2\text{K/W}$.

It has to be noted that to get these results, it has been necessary to increase the second parameter for the wavelet transform to 10.

It can also be noted that, when studying the sliding average value of the instantaneous effectiveness (over a 2000 sample observation window), although the detection can occur sooner, some tests (7%) lead to higher values of the fouling factor at detection, as shown in figure 16. In that case the reference value is the average value for the first

sliding window (ending at sample 3000), and the threshold has to be decreased to 0.85 to get no false alarm.

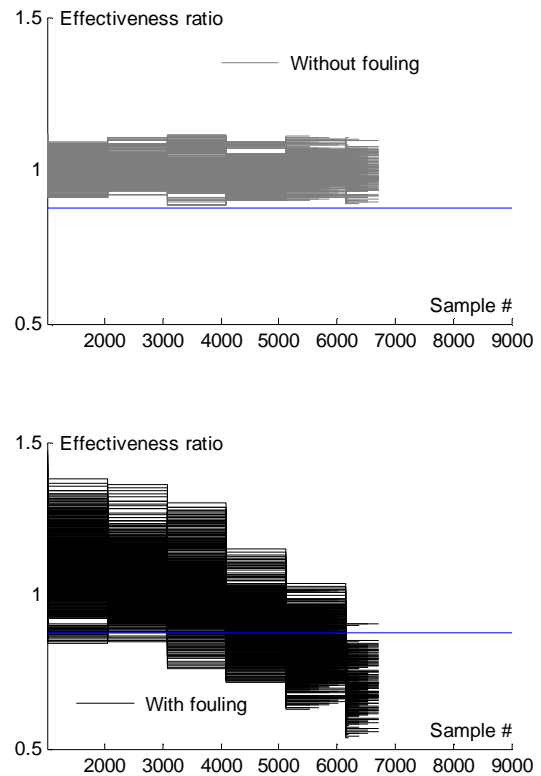


Fig. 15 Evolution of the effectiveness ratio (100 curves) and corresponding detection sample

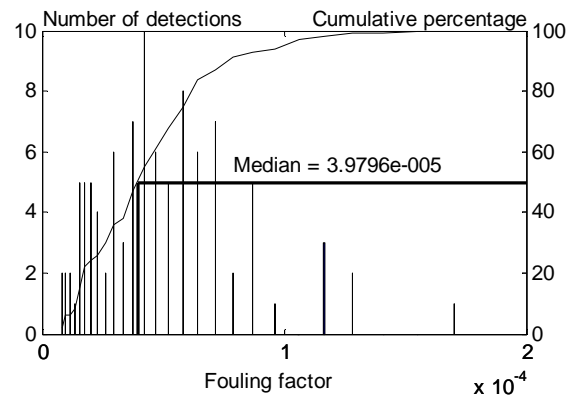


Fig. 16 Distribution of the fouling factor at detection when using a sliding average value

DISCUSSION

Although it could be thought that the wavelet transform is a very complicated tool, it has to be noted that on a up to date personal computer, the approximation of a 10000 sample time series just needs 5.2 ms; using $(\text{dim}, \text{scale}) = (2, 10)$ as done here. It can be concluded that this tool can be implemented online.

The authors think that in real applications, the variation ranges would be much smaller, leading to an even more accurate detection.

CONCLUSIONS

1. In a first part, it has been shown that Simulink can be used to accurately model a cross flow heat exchanger. Then, it has been shown that using wavelets can lead to an early detection of fouling in a heat exchanger. Nevertheless, as it is not based on a sliding window, the method could be computationally burdensome if fouling occurs on a very long period. In that case, the user could get enough data to try to adapt the procedure on sliding windows where the inputs do not vary too much.

2. Tests will be carried out on the test rig under construction at the Université de Valenciennes et du Hainaut Cambrésis. Then the efficiency of various methods (model based identification, neural networks, time series analysis, fuzzy models, ...) will be compared.

ACKNOWLEDGMENTS

Special thanks are due to Mr. A. Chamroo, Mr. G. Mercère, and Mr. T. Poinot, from the "Laboratoire d'Automatique et d'Informatique Industrielle" at the Université de Poitiers for their precious advices for the Simulink implementation of differential equations.

This work could not have been carried out without the financial help of the European Union (Erasmus grant for one author), the French/Icelandic "Jules Verne" program (18990VL), and the DESURENEIR project supported by the CNRS. All these helps are greatly acknowledged.

NOMENCLATURE

A	area of the convection surface, m^2 (or m^2/m when without subscripts)
c	specific heat, $J/kg.K$
dim	first parameter for the wavelet transform
h	convection coefficient, $W/m^2.K$
I_0	modified Bessel function of first kind and of order 0
M	mass of fluid in one cell, kg
\dot{m}	mass flow rate, kg/s
s	Laplace variable
scale	second parameter for the wavelet transform
T	temperature, $^{\circ}C$
t	time, s
α	convection coefficient on the hot side, $W/m^2.K$
β	convection coefficient on the cold side, $W/m^2.K$
γ	lowpass coefficient of the wavelet
η	lowpass filter part of the wavelet
λ	highpass coefficient of the wavelet
μ	highpass filter part of the wavelet

Subscript

c	cold side
h	hot side
I	in the middle of the cell

i	on the left side of the cell number I
J	in the middle of the cell
j	on the bottom side of the cell number J
p	separating plate

Upperscript

\bar{f}	Laplace transform of function f
-----------------------------	-----------------------------------

REFERENCES

- V. Belotti, F. Crenna, R. C. Michelini, G. B. Rossi, Wheel-flat diagnostic tool via wavelet transform, *Mechanical Systems and Signal Processing* 20 (2006), pp. 1953–1966
- Y.A. Çengel, *Introduction to Thermodynamics and Heat Transfer*, Irwin/McGraw-Hill, 1997
- I. Daubechies, Orthonormal bases of compactly supported wavelets, *Communications on Pure and Applied Mathematics*, Vol. 41, N°7, 1988, pp 909-996
- F. Delmotte, S. Delrot, S. Lalot, M. Dambrine, Fouling detection in heat exchangers with fuzzy models, *Proceedings of the 19th International Symposium on Transport Phenomena*, 17-21 August, 2008, Reykjavik, Iceland, on CD-ROM
- O. Farooq, and S. Datta, Phoneme recognition using wavelet based features, *Information Sciences*, 150 (2003), pp. 5-15
- O. Gudmussun, O. P. Palsson, H. Palsson, and S. Lalot, Method to detect fouling in heat exchangers, *The 11th International Symposium on District Heating and Cooling*, Reykjavik, August 31st-September 2nd, 2008
- R. Guérin, G. Ronse, L. Bouvier, P. Debreyne and G. Delaplace, Structure and rate of growth of whey protein deposit from in situ electrical conductivity during fouling in a plate heat exchanger, *Chemical Engineering Science*, Volume 62, Issue 7, April 2007, Pages 1948-1957
- C. Heneghan, S. M. Khanna, A. Flock, M. Ulfendahl, L. Brundin, and M. C. Teich, Investigating the nonlinear dynamics of cellular motion in the inner ear using the short-time Fourier and continuous wavelet transforms. *IEEE Transactions on Signal Processing*, 42(12), (1994), pp. 3335-3352
- G. R. Jonsson, S. Lalot, O. P. Palsson and B. Desmet, Use of extended Kalman filtering in detecting fouling in heat exchangers, *International Journal of Heat and Mass Transfer*, Volume 50, Issues 13-14, July 2007, Pages 2643-2655
- D. J. Kukulka and M. Devgun, Fluid temperature and velocity effect on fouling, *Applied Thermal Engineering*, Volume 27, Issue 16, November 2007, Pages 2732-2744
- S. Lalot and S. Lecoeuche, Online fouling detection in electrical circulation heaters using neural networks, *International Journal of Heat and Mass Transfer*, Volume 46, Issue 13, June 2003, Pages 2445-2457
- S. Lalot, On-line detection of fouling in a water circulating temperature controller (WCTC) used in injection moulding: Part 1: Principles, *Applied Thermal Engineering*, Volume 26, Issues 11-12, August 2006, Pages 1087-1094

S. Lalot, On-line detection of fouling in a water circulating temperature controller (WCTC) used in injection moulding: Part 2: Application, *Applied Thermal Engineering*, Volume 26, Issues 11-12, August 2006, Pages 1095-1105

S. Lalot, O. P. Palsson, G. R. Jonsson, B. Desmet, Comparison of neural networks and Kalman filters performances for fouling detection in a heat exchanger, *International Journal of Heat Exchangers* 1524-5608/Vol VIII(2007) pp 151-168

S. Lalot and G. Mercère, Detection of fouling in a heat exchanger using a recursive subspace identification algorithm, *Proceedings of the 19th International Symposium on Transport Phenomena*, 17-21 August, 2008, Reykjavik, Iceland, on CD-ROM

T.-S. Li, Applying wavelets transform, rough set theory and support vector machine for copper clad laminate defects classification, *Expert Systems with Applications*, 36, (2009), pp.5822-5829

X. Lou, and K. Loparo, Bearing fault diagnosis based on wavelet transform and fuzzy inference, *Mechanical systems and Signal Processing*, 18, (2004), pp. 1077-1095

G. Mercère, H. Pálsson, T. Poinot Linear parameter-varying identification of a cross flow heat exchanger for fouling detection, *International Conference on Heat Exchanger Fouling and Cleaning*, Schladming, Austria, June 14-19, 2009

J. A. Montoya Zegarra, N. J. Leite, R. da Silva Torres, *Journal of Computational and Applied Mathematics*, Volume 227, Issue 2, 15 May 2009, Pages 294-307

S. Prabhakar, A.R. Mohanty, and A.S. Sekhar, Application of discrete wavelet transform for detection of ball bearing race faults, *Tribology International*, 35 (2002), pp. 793-800

M. Prieto, J. Vallina, I. Suarez, Application of a design code for estimating fouling on-line in a power plant condenser refrigerated by seawater, in the proceedings of the ASME-ZSITS International Thermal Science Seminar, 2000, June 11-14, Bled, Slovenia, on CD-ROM

V. Purushotham, S. Narayanan, and S. A.N. Prasad, Multi-fault diagnosis of rolling bearing elements using wavelet analysis and hidden Markov model based fault recognition, *NDT&E International*, 38 (2005), pp. 654-664

C. Riverol and V. Napolitano, Estimation of the overall heat transfer coefficient in a tubular heat exchanger under fouling using neural networks. Application in a flash pasteurizer, *International Communications in Heat and Mass Transfer*, Volume 29, Issue 4, May 2002, Pages 453-457

R. Rosmaninho, F. Rocha, G. Rizzo, H. Müller-Steinhagen and L.F. Melo, Calcium phosphate fouling on TiN-coated stainless steel surfaces: Role of ions and particles, *Chemical Engineering Science*, Volume 62, Issue 14, July 2007, Pages 3821-3831

R. Rosmaninho, G. Rizzo, H. Müller-Steinhagen and L.F. Melo, Deposition from a milk mineral solution on novel heat transfer surfaces under turbulent flow conditions, *Journal of Food Engineering*, Volume 85, Issue 1, March 2008, Pages 29-41

N. Saravanan, K.I. Ramachandran, Fault diagnosis of spur bevel gear box using discrete wavelet features and Decision Tree classification, *Expert Systems with Applications* 36 (2009), pp. 9564-9573

C.K. Sung, H.M. Tai, C.W. Chen, Locating defects of a gear system by the technique of wavelet transform, *Mechanism and Machine Theory* 35 (2000), pp. 1169-1182

J.-D. Wu, J.-J. Chan, Faulted gear identification of a rotating machinery based on wavelet transform and artificial neural network, *Expert Systems with Applications* 36 (2009), pp. 8862-8875

J.-D. Wu, and C.-H. Liu, An expert system for fault diagnosis in internal combustion engines using wavelet packet transform and neural network, *Expert Systems with Applications*, 36, (2009), pp. 4278-4286

J.-D. Wu, C.-C. Hsu, and G.-Z. Wu, Fault gear identification using discrete wavelet transform and adaptive neuro-fuzzy inference, *Expert systems with Applications*, 36, (2009), pp. 6244-6255